

# Estimating broiler heat stress using computer vision and machine learning

Muhammad Iqbal Anggoro Agung<sup>1</sup>, Eko Mursito Budi<sup>2</sup>, Miranti Indar Mandasari<sup>2,3</sup>

<sup>1</sup>Master of Instrumentation and Control, Faculty of Industrial Technology, Institut Teknologi Bandung, Bandung, Indonesia

<sup>2</sup>Department of Engineering Physics, Faculty of Industrial Technology, Institut Teknologi Bandung, Bandung, Indonesia

<sup>3</sup>Building Physics Research Group, Faculty of Industrial Technology, Institut Teknologi Bandung, Bandung, Indonesia

## Article Info

### Article history:

Received Jul 1, 2024

Revised Feb 24, 2025

Accepted Mar 15, 2025

### Keywords:

Broiler chicken

Cluster index

Computer vision

Instance segmentation

Mask R-CNN

Precision livestock farming

Unrest index

## ABSTRACT

To optimize and enhance the efficiency of broiler chicken farming, it is essential to maintain the chickens' welfare, as heat stress can decrease growth efficiency. The temperature-humidity index (THI) is a key indicator used to determine if chickens are experiencing heat stress. Precision livestock farming (PLF) based on computer vision is one method that can assist farmers in continuously and automatically monitoring the condition of their chickens. This research developed a computer vision-based PLF system to observe chickens with CP 707 strain in a commercial farm using the Mask region-based convolutional neural network (Mask R-CNN) method and object tracking algorithms to analyze features such as the cluster index, unrest index, and the distance traveled by broilers. The results indicated that all features tend to inversely correlate with the THI value, with the cluster index showing the most noticeable tendency. Additionally, it was found that external factors, such as the presence of farmers around the observation area, can affect the chickens' behavior, although the cluster index feature is relatively resilient to disturbances if the operator is not captured by the camera. It was concluded that there is a relationship between the features and the THI value; however, these features are not yet sufficient to distinguish the condition of chickens under high and low THI conditions in real-time.

*This is an open access article under the [CC BY-SA](#) license.*



## Corresponding Author:

Eko Mursito Budi

Department of Engineering Physics, Faculty of Industrial Technology, Institut Teknologi Bandung

St. Ganesa No.10, Lebak Siliwangi, Coblong, Bandung, Jawa Barat 40132, Indonesia

Email: mursito@itb.ac.id

## 1. INTRODUCTION

The consumption of poultry meat as a primary source of animal protein globally is expected to increase from 39.4% in 2022 to 40.8% by 2030 [1]. Therefore, maintaining the efficiency of poultry growth is crucial, given the impact of heat stress which can hinder the growth of broiler chickens, especially at 21-22 days of age [2], [3]. The temperature-humidity index (THI) is a measure used to determine the heat stress condition in broilers, based on temperature and humidity values [4], [5]. Previous studies have shown that the optimal THI value for broilers is around 21 °C [4], [5]. Furthermore, guidelines for broiler farming suggest that the optimal THI value for broilers aged 22 days is around 25 °C [6], [7].

Efforts to optimize production efficiency and animal welfare have driven research into precision livestock farming (PLF), which enables continuous and automatic monitoring using various sensors [8]. Image-based approaches have emerged as effective methods to study poultry behavior under varying environmental conditions [9]. These methods provide non-invasive insights into poultry behavior. Recent

studies have utilized computer vision and machine learning technologies to obtain behavioral features in poultry activities. For instance, Joo *et al.* [10] used Mask region-based convolutional neural network (R-CNN) and YOLOv4 models to classify nine chicken postures and behaviors, while Guo *et al.* [11] compared five convolutional neural network (CNN)-based machine learning models to detect four different chicken behaviors. Moreover, Eijk *et al.* [12] evaluated computational resource efficiency in detecting broilers by comparing Mask R-CNN and U-Net models. Additionally, Massari *et al.* [2] evaluated the cluster index and unrest index in broilers under heat stress by segmenting images based on morphological operations, while Lin *et al.* [13] examined the correlation between THI values and chicken movement detected using Faster R-CNN.

Despite several previous studies, there has less research on commercial poultry farms used in the farming industry as most studies have been conducted in a controlled laboratory environment. Factors such as natural sunlight and larger inconsistent numbers of chickens typical in commercial farms have not been considered in previous research. In this research, broiler with CP 707 strain is observed on a commercial farm to explore and analyze the relation between THI values and broiler activities represented as the cluster index, unrest index, and average broiler movement obtained using Mask R-CNN model for instance segmentation to detect individual chickens. Detected chickens are tracked using an object tracking algorithm and the result was compared with previous results to test whether laboratory results can be applied in commercial farms. If successful, these features will be used to develop a system for detecting chicken conditions under heat stress.

## 2. METHOD

In this research, the computer vision-based PLF system architecture shown in Figure 1 was used to obtain segments of each chicken to be tracked. The Mask R-CNN instance segmentation model was proposed as a method to recognize individual chickens due to its good performance in terms of inference speed and segmentation accuracy produced [14]. The segmentation results are used for the tracker, and feature extraction will be carried out in the form of the unrest index, cluster index, and kinematic features such as the average displacement of tracked chickens. Finally, correlation analysis was carried out between the features and the measured THI value. If there is a correlation between the features and the THI value, a supervised learning-based model will be developed in future research to model chicken behavior under heat stress conditions in real-time.

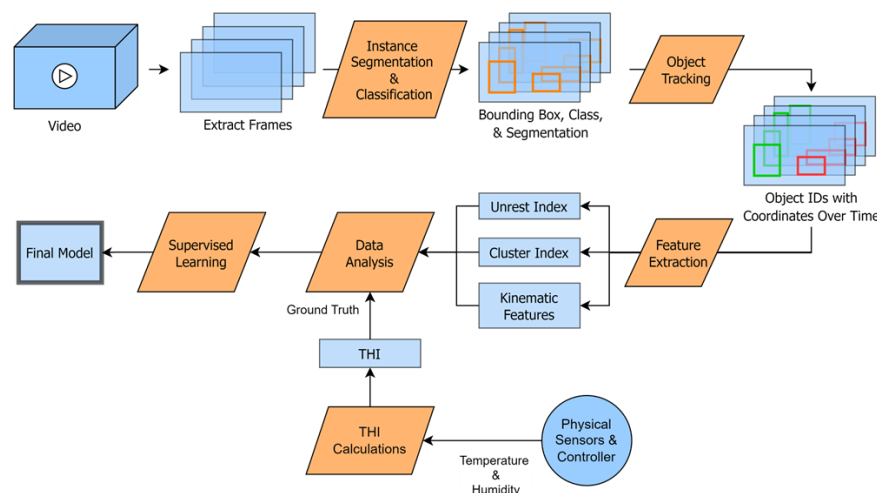


Figure 1. Proposed system architecture for broiler chicken monitoring

### 2.1. Experimental setup

In this study, experiments were conducted in a commercial chicken farm measuring 120×12×2 m located in Subang, West Java, Indonesia. This study observed broilers with strain CP-707 from PT. Charoen Pokphand Indonesia [6]. Broilers were recorded using an IP Camera Uniarch IPC-T124 installed on the ceiling of the farm with a resolution and sampling ratio of 2560×1440@20fps. The IP Camera was positioned as shown in Figures 2(a) and 2(b), capturing the area where chickens consistently stay in frame during the brooding period, including equipment within the farm. The IP cameras were connected to a network video

recorder (NVR) Dahua PFS3010-8ET-96 to record video every day from 06:00 to 20:00 (local time). Industrial temperature and humidity sensors (SM7820B) were connected to a mini-PC server to record data every second. The server time and NVR were then synchronized to a local network time protocol (NTP) server, and all camera and sensor recording data was stored on the server.

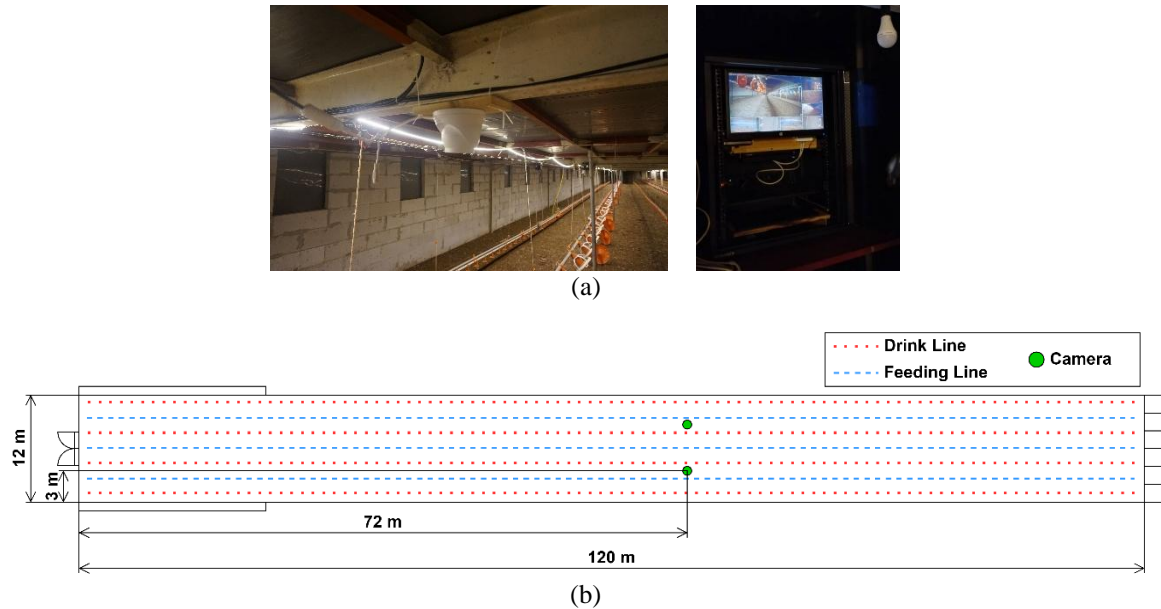


Figure 2. Experiment setup of: (a) camera and server installation and (b) location of camera installation

## 2.2. Data collection and annotation

To train the instance segmentation model, video data recorded from August 19, 2023, to September 23, 2023, was used as the dataset. A sample of 50 images containing broilers and 3 kinds of coop equipment was annotated as shown in Figure 3 using open-source labeling software AnyLabeling. From these sampled images, the dataset was divided into training, validation, and testing, with each set containing data as shown in Table 1. The training set was used to train the model in this research, while the validation set was employed during the training process to evaluate model performance and prevent overfitting. Finally, the testing set was used for the final evaluation after training to assess the performance of the trained model.

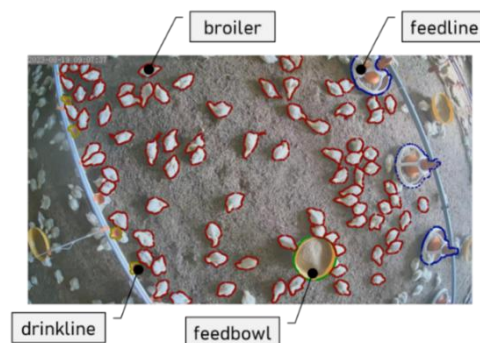


Figure 3. Dataset annotation on 4 classes

Table 1. Dataset splitting

Object	Training (30 Imgs (%))	Validation (10 Imgs (%))	Testing (10 Imgs (%))	Total (50 Imgs (%))
feedbowl	30 (60)	10 (20)	10 (20)	50 (100)
broiler	3,010 (59.54)	1,069 (21.15)	976 (19.31)	5,055 (100)
drinkline	220 (62.14)	67 (18.93)	67 (18.93)	354 (100)
feedline	100 (62.12)	31 (19.25)	30 (18.63)	161 (100)

### 2.3. Instance segmentation and multi object tracking

The segmentation process was conducted by comparing the Mask R-CNN model [14], with the best backbone then used as the tracker for multi-object tracking using an algorithm based on the simple online and realtime tracking (SORT) algorithm [15]. This study utilized a computer running Ubuntu 22.04 operating system with Python 3.11.9 and Pytorch 2.3.0 with GPU support installed. The research was conducted on an PC installed with Processor Intel i7-13700K, 128 GB sized RAM, and an Nvidia GeForce RTX 4070 GPU with 12 GB of memory.

#### 2.3.1. Mask region-based convolutional neural network

Mask R-CNN is an extension of the Faster R-CNN object detection algorithm [16], which incorporates a semantic segmentation algorithm using a fully convolutional network (FCN) [17] on the region of interest (RoI) layer for object segmentation [14]. In this study, the ResNet50 backbone with a feature pyramid network (FPN) [18], as depicted in Figure 4, was utilized. Other than that, ResNet-101-FPN and ResNeXt-101-FPN backbones were trained to compare and evaluate the performance of each backbone model. The training process for each backbone was conducted over 3,000 iterations, with transfer learning using model that had previously been pretrained on the MS COCO dataset were performed to further train the model to recognize broilers using the created dataset. Inference using Mask R-CNN produces outputs such as object segmentation masks, bounding boxes, and object centroid coordinates based on the segmentation results. These outputs were then utilized as the tracker for object tracking using the SORT-based tracking algorithm.

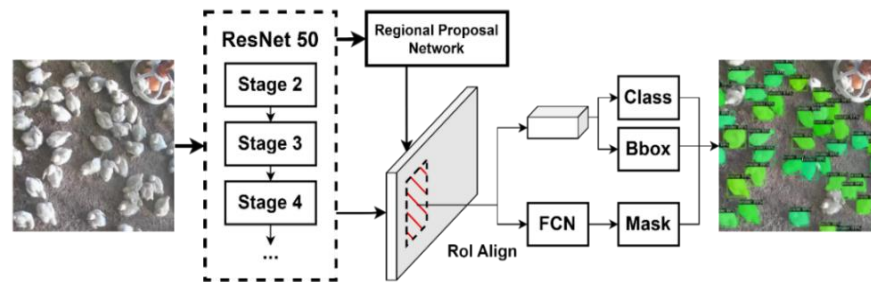


Figure 4. Mask R-CNN architecture

#### 2.3.2. Simple online and realtime tracking

SORT is a multi-object tracking algorithm that utilizes the Kalman filter [19], assuming a constant velocity model for object motion [15]. The Kalman filter is employed to estimate changes in object positions from the previous frame and match them with detections in the current frame. Once matched, these frames are used to update the Kalman filter state [15]. In this study, the tracking process based on the SORT algorithm was implemented using the norfair framework [20], as illustrated in Figure 5.

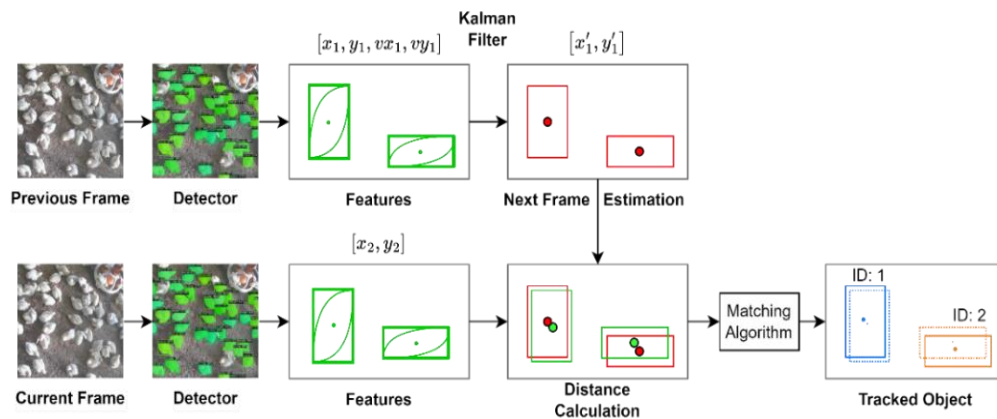


Figure 5. SORT-based tracking algorithm

In this research, the centroid coordinates from the segmentation results of broiler class were used as features for calculating the distance between frames. The closest object distances meeting a specified threshold were used as parameters to match objects across frames. The tracking algorithm outputs object identities along with information of segmentation masks, bounding boxes, and centroid coordinates for each tracked frame.

#### 2.4. Feature extraction

To model broiler conditions during heat stress, feature extraction was performed based on the tracking results. This study focuses on testing and analyzing three features, namely unrest index [21], cluster index [22], and average travel distance [13]. The first feature, unrest index, measures the difference between sets of objects across two frames within a specific time interval, defined by (1).

$$\text{Unrest Index}_{(i,i-1)} = k \cdot dH(F_{(i)}, F_{(i-1)}) \quad (1)$$

Where  $dH$  represents the symmetric Hausdorff distance [23] between sets of centroid coordinates of objects in the current frame  $F_{(i)}$  and the previous frame  $F_{(i-1)}$ .  $k$  is the proportionality factor of the image capture camera, defined by (2).

$$k = \frac{2H \tan(\alpha/2)}{w} \quad (2)$$

The value of the proportionality factor  $k$  depends on the camera height  $H$ , lens aperture angle  $\alpha$ , and the pixel width  $w$  of the charge-coupled device (CCD) sensor. The next feature is the cluster index, which represents how densely objects are clustered at a given time, defined by (3).

$$\text{Cluster Index}_{(i)} = \frac{2 \times \bar{A} \times \sqrt{h^2 + w^2}}{\bar{P} \times \bar{D} \times n_A} - 1 \quad (3)$$

Where  $\bar{A}$  and  $\bar{P}$  are the average area and perimeter of detected object segments,  $h$  and  $w$  are the height and width of the image,  $\bar{D}$  is the average distance between centroids of segments, and  $n_A$  is the number of detected segments. The final feature to be tested is the average travel distance, calculated using (4):

$$\text{Avg. Dist}_{(i,i-1)} = \frac{\sum_{j=1}^{n_A} d(S_{j(i)}, S_{j(i-1)})}{n_A} \quad (4)$$

With  $d$  is the distance function between object segments  $S$  for index  $j$  in frame  $i$  and the previous frame  $(i - 1)$ . Various metrics can be used for  $d$ ; however, in this study, Euclidean distance was used to calculate object displacement between frames.

For the testing process, videos recorded on September 2, 2023, from 06:00 to 20:00 with 22-day-old broilers [2] were selected. This period was chosen to observe and track chicken behavior during heat stress conditions. Tracking was conducted with a sampling interval of 1 second to capture significant changes in broiler behavior. Following feature extraction, further analysis was performed to determine correlations between these features and THI values.

#### 2.5. Temperature-humidity index calculation

THI is a metric developed to assess thermal conditions in livestock. For broiler chickens, THI is typically calculated as a linear combination of dry bulb temperature ( $t_{db}$ ) and wet bulb temperature ( $t_{wb}$ ) with specific weights that depend on the type of livestock being observed. For broilers, THI is defined by (5) [4].

$$THI = 0.85t_{db} + 0.15t_{wb} \quad (5)$$

In this study, the wet bulb temperature ( $t_{wb}$ ) is approximated using the empirical equation given by (6) [24]:

$$t_{wb} = t_{db} \left[ 0.151977(RH\% + 8.313659)^{1/2} \right] + \text{atan}(t_{db} + RH\%) - \text{atan}(RH\% - 1.676331) + 0.00391838(RH\%)^{\frac{3}{2}} \text{atan}(0.023101RH\%) - 4.686035 \quad (6)$$

With  $t_{db}$  is the dry bulb temperature reading from the temperature sensor, and  $RH\%$  is the relative humidity reading from the humidity sensor. These values are used to calculate the wet bulb temperature ( $t_{wb}$ ), which is then used in (5) to determine the THI value in the study.

### 3. RESULTS AND DISCUSSION

#### 3.1. Instance segmentation using Mask R-CNN

The training process for each backbone of the Mask R-CNN model was conducted over 3,000 iterations. Model evaluation was performed using the intersection over union (IoU) metric, defined as the ratio of the intersection to the union of the reference segment ( $S_r$ ) and the predicted segment ( $S_p$ ), in (7).

$$IoU(S_r, S_p) = \frac{S_r \cap S_p}{S_r \cup S_p} \quad (7)$$

IoU ranges from 0 to 1, where a value of 0 indicates no overlap between the segments, while a value of 1 indicates perfect overlap. A prediction is considered a true positive (TP) if it meets three criteria: it has the same class as the reference, the prediction probability exceeds a predefined threshold, and the IoU value exceeds a specified threshold. Model performance was evaluated using the COCO evaluation method, assessing average precision (AP) values at IoU thresholds ranging from 50% to 95% in increments of 5%. In this study, AP evaluation was conducted at IoU thresholds of 50%, 75%, and the mean AP over the range 50-95% mean average precision (mAP) shown in Table 2.

Table 2. Evaluation result from training Mask R-CNN

No	Backbone	Bbox mAP	Bbox AP <sub>50</sub>	Bbox AP <sub>75</sub>	Segm mAP	Segm AP <sub>50</sub>	Segm AP <sub>75</sub>
1	ResNet-50-FPN	74.8	83.5	81.6	75.2	83.5	81.5
2	ResNet-101-FPN	70.6	81.6	79.7	73.2	81.6	80.2
3	ResNeXt-101-FPN	71.6	80.0	76.8	71.3	80.0	77.6

Based on Table 2, for the training process with 3,000 iterations, the best results were achieved with the ResNet-50-FPN backbone, showing a value of 2-3 higher AP compared to the next best backbone. This performance improvement was observed both in bounding box evaluation and segmentation results. The comparison of AP evaluation across IoU threshold variations for each class category is illustrated in Figure 6. Based on Figure 6, it is evident that AP values for each backbone decrease around the IoU region of ~85%. Generally, the AP values for segmentation in the broiler class are better than the AP values for bounding boxes, while for other classes, the AP values for bounding boxes are the same or better than those for segmentation. This indicates that the segmentation results, especially for the broiler class, are more suitable for use as features in the object tracking process.

The model with ResNet-50-FPN as the backbone achieved the best results, particularly for the broiler class, as shown in Figure 6(a). At an IoU threshold of 0.70, the AP values did not show a significant decline. In contrast, models with ResNet-101-FPN and ResNeXt-101-FPN exhibit a notable decline in AP values at the same IoU threshold, as illustrated in Figures 6(b) and 6(c). Among the four classes trained with various backbones, the drinkline class performed the worst, as indicated by its AP values, which were considerably lower than those of the other classes.

Additionally, the findings from the visualization results of the segmentation models show that the ResNet-50-FPN backbone (Figure 6(a)) produces better results with fewer errors compared to other backbones. Other backbones (Figures 6(b) and 6(c)) exhibit significant errors. These include incorrectly detecting parts of the operator captured on camera. Which are less pronounced with the ResNet-50-FPN backbone.

#### 3.2. Feature comparison with THI

After the segmentation process was successfully conducted, feature values were calculated using (1) to (4), and the THI values were computed using (5) and (6). Figure 7(a) shows the THI graph in blue, while the bar graph represents the histogram of normalized average values for each feature to facilitate visualization and observation, with a 95% confidence interval (CI). It can be observed that between approximately 9:30 and 14:30, there were fluctuations in THI values due to the automatic control system in the farm, which activated the cooling pump to cool the incoming air as the THI inside the farm rose too high, reaching up to 30 °C.

Based on the observation of the features, the cluster index generally exhibited an inverse relationship with the THI values, especially at the beginning when the THI values were very low, consistent with the findings of Pereira's [22] research. The unrest index also showed an inverse trend, though it was less pronounced compared to the cluster index. This difference is attributed to the less significant temperature variation within the farm, aligning with the findings of Valle *et al.* [21], who noted that the unrest index for broilers showed significant changes at temperatures around 35 °C, corresponding to THI values of



approximately 33 to 34 °C. The average displacement index was primarily noticeable between 08:00 and 16:00, with a distribution similar to the findings of Lin *et al.* [13].

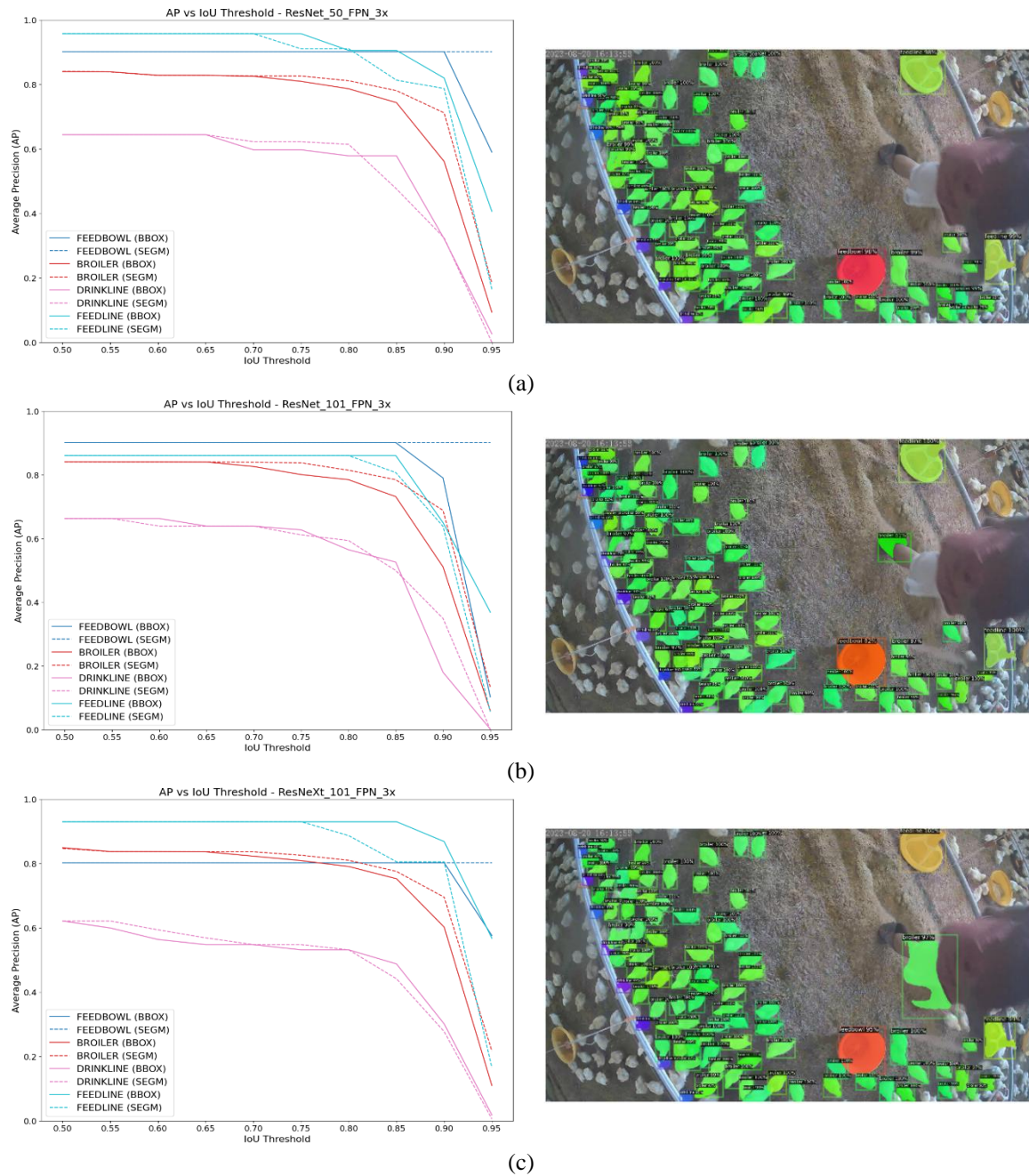


Figure 6. Comparison of backbones (a) ResNet-50-FPN, (b) ResNet-101-FPN, and (c) ResNeXt-101-FPN

A deeper analysis of the index data sampled per second, as shown in Figure 7(b), revealed several instances where feature values significantly increased. Further analysis and observation of the video recordings indicated that these peaks corresponded to instances where an operator or farmer entered the farm and was captured on camera, as illustrated in Figure 8. Other peaks in the average displacement feature were due to sudden and simultaneous movements of the chickens, triggered by the presence of a farmer or operator not captured by the camera. This suggests that the cluster index and unrest index features are more resilient to external disturbances caused by farmers or operators in the data collection area compared to the average displacement.

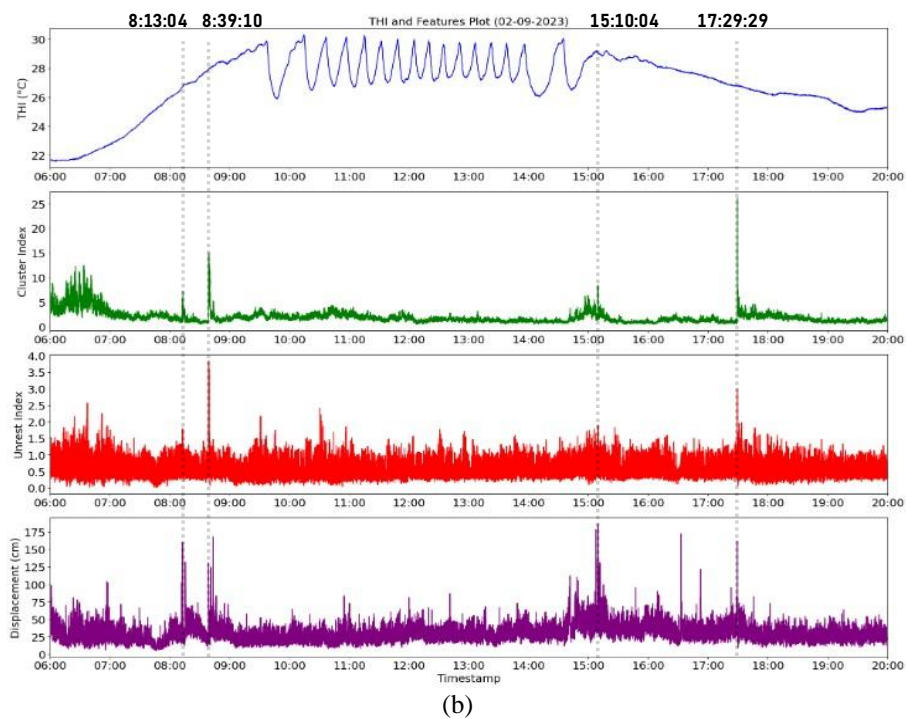
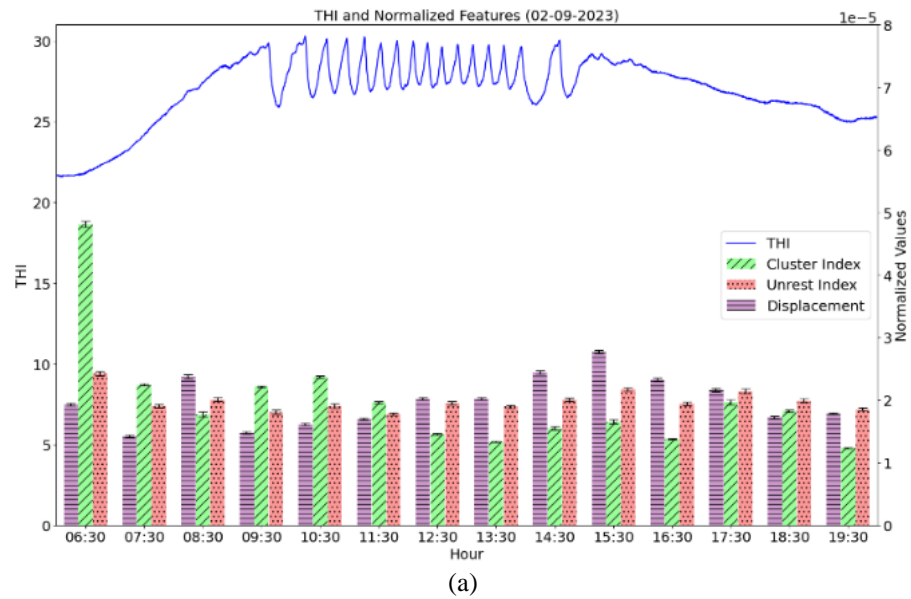


Figure 7. THI calculation (a) cumulative (b) sampled every second



Figure 8. Example of operator captured on camera



The cluster index is more resistant to disturbances because its calculation is not based on two different frame conditions. The cluster index value only increases if the farmer or operator is captured by the camera, causing many chickens to move away and not be captured. A reduced number of chickens ( $n_A$ ) results in a minimum value in the denominator of (3), leading to an increase in the cluster index value. If the farmer or operator is not captured by the camera, the cluster index value is not significantly affected even if the chickens move, because they are still detected and captured by the camera.

In contrast, both the unrest index and average displacement features depend on the comparison between the two frames. Whether the operator is captured or not, if the operator or farmer is near the chickens and causes increased movement, both index values will rise. When comparing the unrest index and average displacement, the unrest index is more resistant to disturbances because it uses the Hausdorff distance, which only compares the spread of central points between two frames without considering the identity of each object. For example, if two objects switch positions between two frames, the unrest index calculation, which does not account for the identity of each object, results in a minimal Hausdorff distance evaluation due to the nearly identical positions. In contrast, the average displacement calculation tracks the movement of objects by maintaining the same identity; thus, when positions are switched, there is still displacement, resulting in a non-zero displacement value. To analyze further whether these three features can classify the condition of chickens under heat stress, an exploratory data analysis (EDA) of the features was conducted by plotting mean of each features on each THI range, calculating Pearson correlation matrix [25] to determine linear correlation between the variables, and lastly plotting all the features on 3D scatter plot, with THI values as the heatmap of the data point.

Figure 9 shows mean of each feature on different THI ranges, having negative trend on cluster index and unrest index which align with the results from previous research [2], [21], [22], while displacement shows negative trend in low temperatures and positive trend on middle and higher temperature. This happens because there was disturbance from the operators which made the chickens move. Hence further data processing such as data cleaning or filtering were needed to process the data for further use.

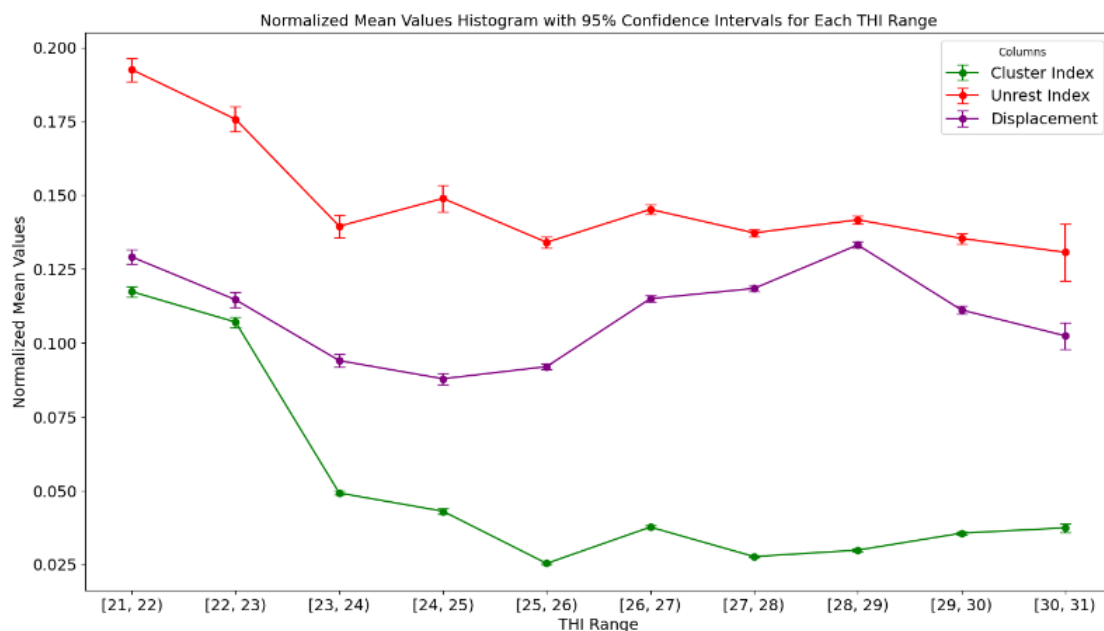


Figure 9. Normalized features mean on different THI range

The Pearson correlation matrix in Figure 10 shows that cluster index having a negative correlation with value of -0.5 with THI while the other two have a low correlation with THI. This means that cluster index has some linear correlation inversely to some extent with THI, which correspond with the results from Figure 7. Unrest index also has a negative correlation with low value, indicating that these features are have an inverse correlation, but not linearly correlated with THI. Similar results show on the displacement feature that have very low correlation with THI, because of the same disturbance by the operators around the observation area.

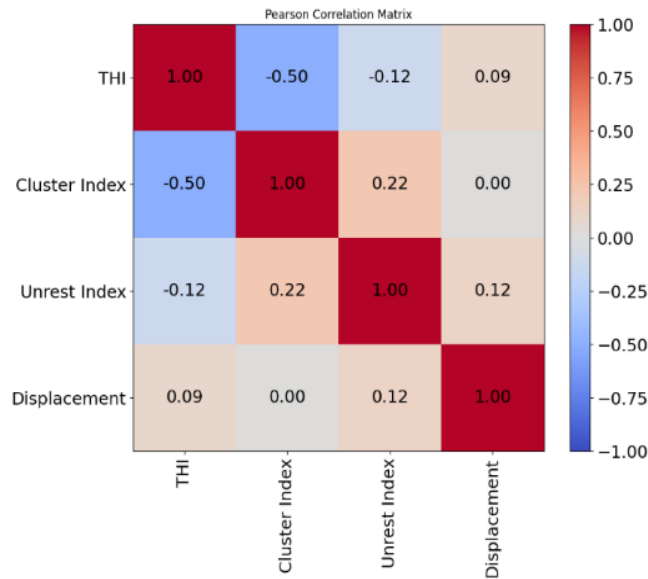


Figure 10. Pearson correlation matrix of THI and each feature

Figures 11(a) and 11(b) show that conditions with high (red) and low (blue) THI values are quite overlapping, making it difficult to distinguish the chicken's condition under high and low THI. However, the direction of cluster index axis stands out as it can better differentiate between high and low THI conditions. Compared to the other two axis, with better visibility of the separation between red and blue color.

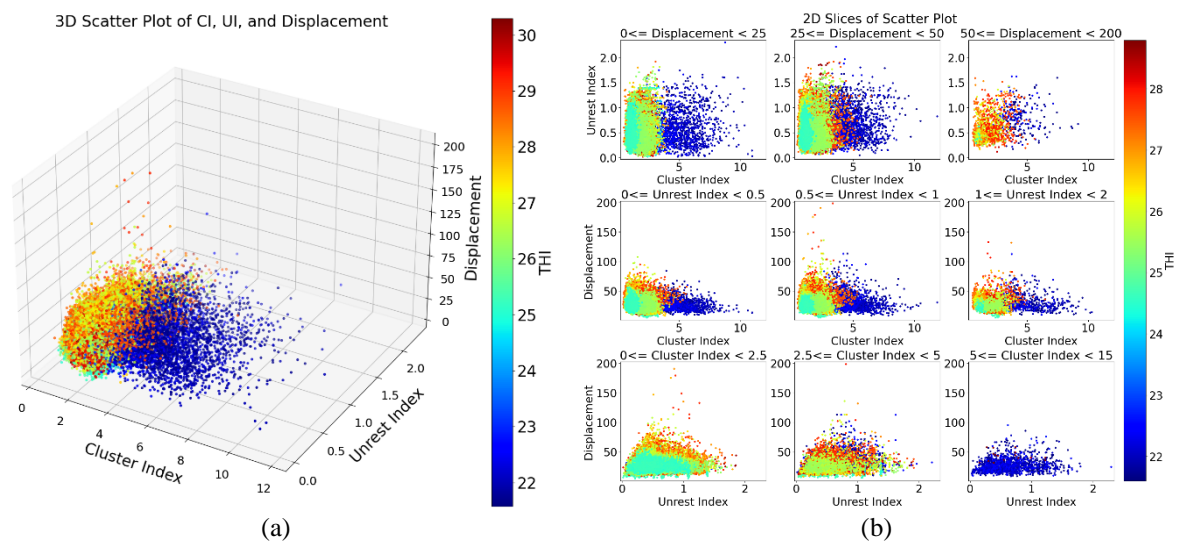


Figure 11. Scatter plot of 3 features on (a) 3D Scatter Plot and (b) 2D Slice of the 3D plot

Based on the findings, all three features are related to the chickens' conditions under high and low THI, as observed in the cumulative evaluation results in Figure 7(a). However, a more in-depth analysis reveals that it's not yet clear if these features alone are sufficient for real-time chicken condition recognition. From Figures 7, 9, and 11, the cluster index feature appears to have a better capability to distinguish chicken conditions under high and low THI compared to the other two features.

The data segmentation process in this study, by using the Mask R-CNN method may influence feature extraction. Previous studies used mathematical segmentation methods like filtering, mathematical morphology operations, and binarization for feature extraction of the cluster index and unrest index [2], [21], [22]. These methods allow for consistent detection of chickens as long as they have a distinct color contrast from

the background and consistent lighting, while there were no other objects with similar color with the chickens. However, in commercial farms, lighting conditions cannot be consistently maintained due to external factors, and some visual disturbances like the presence of the operators captured on camera, making the Mask R-CNN method a viable solution for commercial farm applications. Caution is needed with Mask R-CNN, as poorly trained models can result in misdetections, either falsely identifying non-chickens as chickens or failing to detect chickens.

Furthermore, previous feature testing was conducted in laboratory-scale farms with a small number of chickens and small farm sizes, ensuring all chickens and the farm were captured by the camera [2], [13], [21], [22]. This setup minimizes the chance of chickens moving in and out of the camera's field of view, maintaining a consistent number of chickens for feature calculations. In commercial farm applications, chickens' free movement can lead to extreme conditions, such as no chickens or very high numbers of chickens being captured, affecting feature calculations. External factors like operators entering the farm can also influence chicken behavior, indicating the need for further development in recognizing chicken behavior relative to THI changes.

To apply this system in commercial farms, further development could include additional features like sound detection [26], which could improve behavior recognition accuracy. Additionally, more research on the use of cluster index and unrest index in commercial farm conditions is necessary. This study aims to pave the way for further development of PLF in recognizing heat stress in chickens, potentially helping farmers improve livestock quality in commercial settings.

#### 4. CONCLUSION

This research explores the potential of applying a computer vision-based PLF system using Mask R-CNN to estimate the chicken heat stress under different THI conditions. Several Mask R-CNN backbones were trained and compared, demonstrating their ability to effectively identify broilers and equipment in the coop. Feature extraction from the best-performing backbone included cluster index, unrest index, and average displacement, which were analyzed for their correlation with THI. The analysis revealed that these features have a relationship with THI values, with the cluster index emerging as the best feature for correlating with THI. However, further development of these features is necessary for effective application in commercial farms.

#### ACKNOWLEDGMENTS

Author thanks Nantara Farm for providing the commercial farm as the research site.

#### FUNDING INFORMATION

This study was funded by the Kedaireka Matching Fund Program in 2023 under contract number 73/E1/HK.02.02/2023 from the Ministry of Education, Culture, Research, and Technology of Indonesia.

#### AUTHOR CONTRIBUTIONS STATEMENT

This journal uses the Contributor Roles Taxonomy (CRediT) to recognize individual author contributions, reduce authorship disputes, and facilitate collaboration.

Name of Author	C	M	So	Va	Fo	I	R	D	O	E	Vi	Su	P	Fu
Muhammad Iqbal	✓	✓	✓	✓	✓	✓		✓	✓	✓	✓			
Anggoro Agung														
Eko Mursito Budi	✓	✓		✓	✓	✓	✓	✓	✓	✓		✓	✓	✓
Miranti Indar		✓		✓						✓		✓	✓	
Mandasari														

C : **C**onceptualization

M : **M**ethodology

So : **S**oftware

Va : **V**alidation

Fo : **F**ormal analysis

I : **I**nterpretation

R : **R**esources

D : **D**ata Curation

O : **O**riginal Draft

E : **E**diting

Vi : **V**isualization

Su : **S**upervision

P : **P**roject administration

Fu : **F**unding acquisition

## CONFLICT OF INTEREST STATEMENT

The authors declare that they have no known competing financial interests or personal relationships that could have appeared to influence the work reported in this manuscript. Furthermore, the authors confirm that there are no affiliations with or involvement in any organization or entity with any financial, personal, professional, political, religious, ideological, academic, or intellectual interest in the subject matter or materials discussed in this manuscript that could be perceived as a potential conflict of interest. Regarding those matters, authors state no conflict of interest.

## ETHICAL APPROVAL

The videos of the broilers used in this study were taken in a legally operating chicken coop and have complied with all the relevant national regulations and institutional policies for the care and use of animals.

## DATA AVAILABILITY

In line with our commitment to research transparency and reproducibility, the availability of data supporting the findings of this study is described below:

- The data that support the findings of this study are available on request from the corresponding author, [EMB]. The data, which contain information that could compromise the privacy of research participants, are not publicly available due to certain restrictions.
- Derived data supporting the findings of this study are available from the corresponding author [EMB] on request.





## REFERENCES

- [1] OECD/FAO, *OECD-FAO agricultural outlook 2021-2030*, Paris, France: OECD Publishing, 2021, doi: 10.1787/19428846-en.
- [2] J. M. Massari, D. J. D. Moura, I. D. A. Nääs, D. F. Pereira, and T. Branco, "Computer-vision-based indexes for analyzing broiler response to rearing environment: a proof of concept," *Animals*, MDPI, vol. 12, no. 7, pp. 1-12, Mar. 2022, doi: 10.3390/ani12070846.
- [3] I. Andretta, M. Kipper, G. D. Schirmann, C. S. Franceschina, and A. M. L. Ribeiro, "Modeling the performance of broilers under heat stress," *Poultry Science*, vol. 100, no. 9, 2021, doi: 10.1016/j.psj.2021.101338.
- [4] X. Tao and H. Xin, "Temperature-humidity-velocity index for market-size broilers," in *2003 ASAE Annual Meeting*, 2003, doi: 10.13031/2013.14094.
- [5] J. L. Purswell, W. A. Dozier, H. A. Olanrewaju, J. D. Davis, H. Xin, and R. S. Gates, "Effect of temperature-humidity index on live performance in broiler chickens grown from 49 to 63 days of age," in *ASABE - 9th International Livestock Environment Symposium 2012, ILES 2012*, 2012, pp. 41-49, doi: 10.13031/2013.41619.
- [6] PT. Charoen Pokphand Jaya Farm, *Manual management broiler CP 707*, Jakarta, Indonesia: PT. Charoen Pokphand Jaya Farm - Poultry equipment, 2014.
- [7] COBB, *Optimum broiler development: a practical guide to ensure correct early broiler performance*, Siloam Springs, United States: COBB Vantres, 2015.
- [8] D. Berckmans, "Automatic on-line monitoring of animals by precision livestock farming," in *Livestock Production and Society*, BRILL Publishing, 2006, pp. 287-294, doi: 10.3920/9789086865673\_023.
- [9] N. Li, Z. Ren, D. Li, and L. Zeng, "Review: automated techniques for monitoring the behaviour and welfare of broilers and laying hens: towards the goal of precision livestock farming," *Animal*, vol. 14, no. 3, pp. 617-625, 2020, doi: 10.1017/S1751731119002155.
- [10] K. H. Joo, S. Duan, S. L. Weimer, and M. N. Teli, "Birds' eye view: measuring behavior and posture of chickens as a metric for their well-being," *arXiv-Computer Science*, pp. 1-12, 2022.
- [11] Y. Guo, S. E. Aggrey, P. Wang, A. Oladeinde, and L. Chai, "Monitoring behaviors of broiler chickens at different ages with deep learning," *Animals*, vol. 12, no. 23, 2022, doi: 10.3390/ani12233390.
- [12] J. A. J. van der Eijk *et al.*, "Seeing is caring – automated assessment of resource use of broilers with computer vision techniques," *Frontiers in Animal Science*, vol. 3, 2022, doi: 10.3389/fanim.2022.945534.
- [13] C. Y. Lin, K. W. Hsieh, Y. C. Tsai, and Y. F. Kuo, "Monitoring chicken heat stress using deep convolutional neural networks," in *ASABE 2018 Annual International Meeting*, 2018, doi: 10.13031/aim.201800314.
- [14] K. He, G. Gkioxari, P. Dollár, and R. Girshick, "Mask R-CNN," *arXiv-Computer Science*, pp. 1-12, 2017.
- [15] A. Bewley, Z. Ge, L. Ott, F. Ramos, and B. Upcroft, "Simple online and realtime tracking," in *2016 IEEE International Conference on Image Processing (ICIP)*, 2016, pp. 3464-3468, doi: 10.1109/ICIP.2016.7533003.
- [16] S. Ren, K. He, R. Girshick, and J. Sun, "Faster R-CNN: towards real-time object detection with region proposal networks," *arXiv-Computer Science*, pp. 1-14, 2015.
- [17] J. Long, E. Shelhamer, and T. Darrell, "Fully convolutional networks for semantic segmentation," *arXiv-Computer Science*, pp. 1-10, 2015.
- [18] T.-Y. Lin, P. Dollár, R. Girshick, K. He, B. Hariharan, and S. Belongie, "Feature pyramid networks for object detection," *arXiv-Computer Science*, pp. 1-10, 2017.
- [19] R. E. Kalman, "A new approach to linear filtering and prediction problems," *Journal of Basic Engineering*, vol. 82, no. 1, pp. 35-45, 1960, doi: 10.1115/1.3662552.
- [20] J. Alori *et al.*, "Tryolabs/norfair," *Zenodo*, vol. v2.2.0, 2023, doi: 10.5281/zenodo.7504727.
- [21] J. E. D. Valle, D. F. Pereira, M. Mollo Neto, L. R. A. Gabriel Filho, and D. D. A. Salgado, "Unrest index for estimating thermal comfort of poultry birds (*Gallus gallus domesticus*) using computer vision techniques," *Biosystems Engineering*, vol. 206, pp. 123-134, 2021, doi: 10.1016/j.biosystemseng.2021.03.018.





- [22] D. F. Pereira, F. A. A. Lopes, L. R. A. G. Filho, D. D. A. Salgado, and M. M. Neto, "Cluster index for estimating thermal poultry stress (*gallus gallus domesticus*)," *Computers and Electronics in Agriculture*, vol. 177, Oct. 2020, doi: 10.1016/j.compag.2020.105704.
- [23] A. A. Taha and A. Hanbury, "An efficient algorithm for calculating the exact hausdorff distance," *IEEE Transactions on Pattern Analysis and Machine Intelligence*, vol. 37, no. 11, pp. 2153–2163, 2015, doi: 10.1109/TPAMI.2015.2408351.
- [24] R. Stull, "Wet-bulb temperature from relative humidity and air temperature," *Journal of Applied Meteorology and Climatology*, vol. 50, no. 11, pp. 2267–2269, 2011.
- [25] J. L. Rodgers and W. A. Nicewander, "Thirteen ways to look at the correlation coefficient," *The American Statistician Association*, vol. 42, no. 1, pp. 59–66, 2012.
- [26] J. Lee, B. Noh, S. Jang, D. Park, Y. Chung, and H. H. Chang, "Stress detection and classification of laying hens by sound analysis," *Asian-Australasian Journal of Animal Sciences*, vol. 28, no. 4, pp. 592–598, 2015, doi: 10.5713/ajas.14.0654.

## BIOGRAPHIES OF AUTHORS







**Muhammad Iqbal Anggoro Agung**     currently a master student at Department of Instrumentation and Control, Institut Teknologi Bandung, expected to graduate in 2024. He holds a Bachelor of Science in Engineering Physics from Faculty of Industrial Technology, Institut Teknologi Bandung. He has interest in internet of things, data science, and machine learning, especially in computer vision. He can be contacted at email: 23822005@mahasiswa.itb.ac.id or aangiqbal26@gmail.com.



**Eko Mursito Budi**     is an associate professor in the Faculty of Industrial Technology, Institut Teknologi Bandung. He is a multi-disciplinary engineer with various innovations, including virtual control, real-time object-oriented kernel, angklung robot, and batik photonics. He had undergraduate and doctoral degrees in the Engineering Physics Program and a master's degree in Informatics. He can be contacted at email: mursito@itb.ac.id.



**Miranti Indar Mandasari**     received her bachelor's degree in 2008 and her master's degree in 2010, both from Institut Teknologi Bandung, Indonesia. She completed her Ph.D. in 2018 at Radboud University Nijmegen, Netherlands. She is currently a lecturer in Department of Engineering Physics, Faculty of Industrial Technology, Institut Teknologi Bandung. She has interest in data science, speaker recognition, likelihood ratio calibration, forensics, and biometrics. She can be contacted at email: mandasari@itb.ac.id.